Study of transition regime for amorphous to nano-crystalline silicon thin films using 27.12 MHz PECVD: Insight into plasma kinetics

Deepika Chaudhary[1, 2], Mansi Sharma[1, 2], S. Sudhakar[1], Sushil Kumar[1, 2*]

[1]*Network of Institutes for Solar Energy (CSIR-NISE), Physics of Energy Harvesting Division, CSIR – National Physical Laboratory, New Delhi 110012, India*
[2]*Academy of Scientific and Innovative Research (AcSIR), CSIR-NPL Campus, New Delhi, Dr. K. S. Krishnan Marg, New Delhi 110012, India*

[*]Corresponding author: E-mail: skumar@mail.nplindia.org; Tel: (+91) 11 45608650; Fax: (+91) 11 45609310

Received: 30 March 2016, Revised: 01 August 2016 and Accepted: 19 April 2017

DOI: 10.5185/amp.2017/644
www.vbripress.com/amp

Abstract

In this article, we report the phase transition region of hydrogenated amorphous (a-Si:H) to nano-crystalline (nc-Si:H) silicon thin films deposited using 27.12 MHz assisted Plasma Enhanced Chemical vapor Deposition (PECVD) process with the approach of plasma diagnosis. This work presents for the first time a study of plasma characteristics using Impedance Analyser (V/I probe) at various applied power (4 W - 40 W), though till now this apparatus has been utilized only to analyse the applied delivered power during processing. On the basis of plasma diagnose, optimum bulk field (5 V/cm); sheath field (1376 V/cm) and minimum sheath width (7.4×10^{-4} cm) observed at 20 W power which provides a visible mark of transition from a-Si:H to nc-Si:H. On account of plasma properties, the deposition was carried out by considering the plasma-surface interaction during growth. The microstructure of the deposited films was characterized using Raman spectra, UV-Vis spectra and conductivity measurements and they were found to be well correlating with the evaluated plasma characteristics. In particular, it was found that at applied power near to the onset of transition regime i.e. at 10 W, preeminent properties of a-Si:H film was observed, predominantly in terms of highest photosensitivity (7.2×10^{3}), low photo-degradation and high deposition rate (~1.39 Å/s). On the other hand, volume fraction of crystallites (24 %), wider band gap (2.0 eV) and no photo-degradation observed for the film deposited at 20 W applied power which signifies the existence of crystallites in an amorphous matrix. Copyright © 2017 VBRI Press.

Keywords: 27.12 MHz assisted PECVD process, transition region, plasma diagnostics, a-Si:H film, nc-Si:H thin film.

Introduction

Hydrogenated nano-crystalline silicon (nc-Si:H) thin film has attracted considerable attention due to its ability to absorb long wavelength photons in visible and infrared region, higher mobility because of its rigid structure and its better stability under prolonged light soaking as compared to the basic material of silicon thin film i.e. hydrogenated amorphous silicon (a-Si:H) [**1**]. nc-Si:H is the biphasic material; it consists of nano-meter size crystals surrounded by amorphous matrix. Thus, nano-crystalline is a promising material for the thin film transistors (TFT), liquid crystal display (LCD), Tandem solar cell structure, etc [**2**, **3**]. The most common method for the growth of silicon thin films is Plasma Enhanced Chemical Vapor Deposition (PECVD) process where the deposition conditions affect the properties of the film. In this process, plasma dissociates the precursor gas like Silane (SiH_4), after that these dissociated species accelerates toward the substrate by following the gas phase reaction, and thus, deposition takes place. In the PECVD process, amalgamation of nc-Si:H is not extensively different from amorphous material, nevertheless the transition region from a-Si:H to nc-Si:H influenced by number of deposition parameters, such as chamber pressure, applied power, SiH_4 flow, substrate temperature, ratio of H_2/SiH_4, use of high excitation frequency instead of conventional frequency (13.56 MHz), etc [**4-8**]. Furthermore, for a deviation in any of the parameters the transition regime tends to shift. Thus, how to diagnose this transition is a critical issue for silicon thin film. One can predict this transition with the help of characterization techniques, however these techniques are time consuming procedure requiring a large number of experiments to deposit samples and characterize them to obtain optimized nc-Si:H film.

Taking this into account, simple practical approach derived from plasma measurements was proposed for the prediction of transition zone, based on the idea that the transition regime depends on the change in plasma properties. In this work, we used impedance analyser (V/I probe) for the detection of transition zone, as it is non-intrusive technology which monitors discharge voltage (V_{rms}), current (I_{rms}), plasma impedance (Z) and phase angle (ϕ). However, till now this apparatus was used only to analyse the applied power delivering during processing.The aim of the present work is to explain the preferred plasma conditions to obtain nc-Si:H deposition through plasma diagnosis for $SiH_4 + H_2$ plasma discharge at various applied power using excitation frequency 27.12 MHz. On account of these results, depositions of a-Si:H/nc-Si:H were carried out by varying the applied power. Subsequently the structural, electrical and optical properties of the film were correlated with the plasma analysis, in particular, electron density, bulk field and sheath field which is a concurrent approach for identification of transition region from amorphous to nc-Si:H thin film deposit under 27.12 MHz frequency assisted PECVD process.

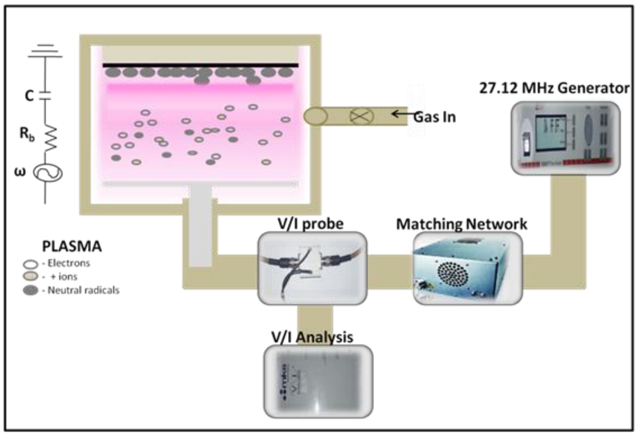

Fig. 1. Schematic representation of PECVD Chamber connected with V/I probe.

Experimental

Material details and synthesis

A capacitively coupled 27.12 MHz assisted PECVD system having an electrode area and inter-electrode gap of 113 cm^2 and 1.2 cm was used for plasma diagnostic though Impedance analyser (MKS – 350 series) and deposition of a-Si:H/nc-Si:H films. The impedance analyser (also known as V/I probe) is an ex-situ real time measurement technique, in which probe was mounted between the power electrode and matching network of excitation frequency to record discharge voltage (V_{rms}), discharge current (I_{rms}), phase difference (Φ) and impedance (Z) of plasma discharge by MKS analysis unit through the software controlled via computer. **Fig. 1** demonstrates the layout of process chamber and plasma analysis unit. Prior to experiment, chamber was evacuated to 10^{-8} Torr using turbo-molecular pump, subsequently source gas SiH_4 (5%) diluted in H_2 (99.999% purity) was fed in the chamber on flow rate of 47 sccm and pressure of 500 mTorr. Flow rate and chamber pressure of SiH_4 was controlled using mass flow controller and Baratron gauge. Thereafter, power was applied from 4 W to 40 W while keeping other process parameters constant to record plasma electrical signals (V_{rms}, I_{rms}, Φ and Z) in the computer. By recording these signals, other plasma parameters such as average electron density, bulk field, sheath field and sheath width can be evaluated to study the effect of power on plasma characteristics. On account of these results, deposition were carried out at 270°C substrate temperature on two different substrates, Corning 7059 glass and double sided polished <100> Silicon wafer, simultaneously.

Plasma characterization

Plasma discharge is divided into two regions (1) Bulk plasma where positive ions and radicals are formed due to disassociation of Silane gas by electron collision, and (2) Sheath plasma generates due to mobility difference between electron and ions. The ions and radicals arrive at the substrate through sheath and undergo surface reaction in deposition. In this work, the "capacitive sheath model" was used, wherein plasma discharge represented as an equivalent series of discharge capacitance, $C = I_{rms}/(\omega * V_{rms} * \sin\Phi)$ and discharge resistive component, $R_b = (V_{rms} * \cos\Phi)/I_{rms}$ [**9**]. Here, C and R_b in the plasma directly associated with the sheath properties such as sheath width and sheath field, and bulk properties such as average electron density and bulk field, respectively.

Film characterization

The film thickness was measured using stylus profilometer (NanoMap 500ES) to estimate deposition rate (film- thickness/deposition-time). Raman spectra were recorded in the back scattering mode at room temperature using Raman microprobe in which the 514.5 nm laser radiation was obtained from an Argon laser. The power of the incident beam was set as low as possible to avoid laser induced crystallization. For nano-crystalline silicon film, the crystalline fraction can be obtained by de-convoluting the spectra in the wave-number range 300-650 cm^{-1} into three Lorentzian peaks defined by, $Xc = \frac{I_c}{I_c + I_g + I_a}$, where I_c, I_g and I_a are the integrated area of crystalline (peak position ~ 520 cm^{-1}), grain boundaries (~ 490 cm^{-1}) and amorphous (~ 480 cm^{-1}) dominated region [10]. The average crystallite size calculated by the expression $D = 2\pi\ (B/\Delta\omega)^{1/2}$, where $\Delta\omega$ is the peak shift for the nc-Si:H compared to c-Si (520 cm^{-1}) and B is 2.0 nm^2cm^{-1} [**11**]. Band gap was evaluated considering the procedure of Tauc's plot using UV-Vis transmission measurement by extrapolating the tangent to the curve on x-axis, the intercept of which gives the value of material band gap. $\sqrt{\alpha h\vartheta} = B(h\vartheta - \mathrm{Eg})$, where α, B, E_g and hυ are the absorption coefficient, pre-factor, band gap and photon energy respectively [**12**]. Dark conductivity of the deposited films was measured in the temperature range 298 to 473 K using a Keithley electrometer with coplanar Al contact geometry having a gap of 0.078 cm. Light soaking measurement was made for 600 min. using the coplanar geometry under white light illumination of intensity~100 mW/cm^2.

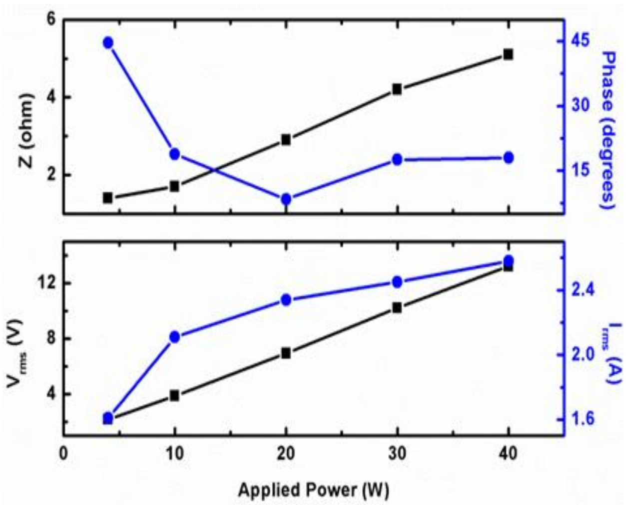

Fig. 2. Variation of discharge voltage (V_{rms}) and current (I_{rms}), Phase difference (ϕ) and Impedance (Z) with applied power.

Results and discussion

Variation Electrical measurement of plasma was performed using V/I probe under different applied power (4 W - 40 W). **Fig. 2** presents the variation of the V_{rms}, I_{rms}, Φ and Z which is necessary for understanding of the plasma behavior as a function of applied power. From here it has been observed that V_{rms} I_{rms} and Z increases with the increase in applied power whereas a drop in the phase angle was observed with a dip at 20 W applied power. The electron and ion dynamics might be the possible reason for this observation which can be further understood with the estimation of the remaining plasma parameters.

As mentioned above, discharge Resistive component (R_b) of plasma is a significant factor and associated with the average electron density (n_e) and bulk field. The n_e and discharge resistance (R_b) related as [**9**],

$$n_e = \frac{\upsilon * d_b * m_e}{R_b * A * e^2} \tag{1}$$

where, m_e is the mass of the electron, d_b is the bulk length, *A* is the discharge cross section area (113 cm^2), e is the electronic charge and υ is the electron momentum transfer collision frequency which can be calculated using a Boltzmann equation solver (Bolsig+) software [13] for gas density 1.7 x 10^{16} cm^{-3} at 500 mTorr process pressure and 270ºC chamber temperature. The estimated values of υ were 4.9 x 10^8 Torr^{-1}s^{-1}, 7.2 x 10^8 Torr^{-1}s^{-1}, 1.1 x 10^9 Torr^{-1}s^{-1}, 2.5 x 10^9 Torr^{-1}s^{-1} and 3.8 x 10^9 Torr^{-1}s^{-1} for 4 W- 40 W applied power. Inter electrode space (12 mm) was taken as d_b. The calculated value of average electron density was depicted in **Fig. 3**. υ and R_b was found to increase with increase in applied power that might be the possible reason for the observed trend of electron density. Since n_e will robustly influence the SiH_4 dissociation rate which thus affect the bulk field (E_b). E_b in the plasma generated due to electron impact dissociation of Silane gas and this is also responsible for the diffusion/drift of radicals/ions towards the sheath region. The E_b can be estimated using [**14**],

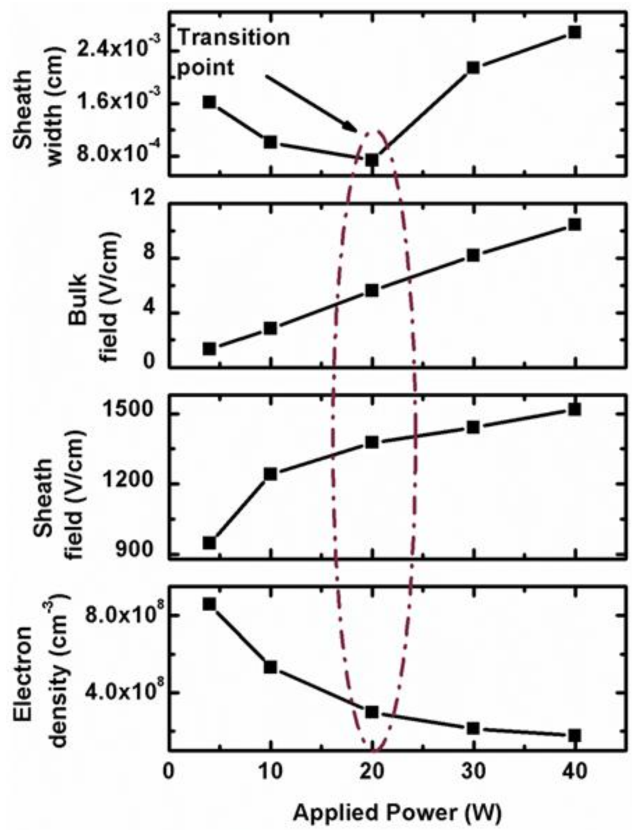

Fig. 3. Variation of electron density, bulk field, Sheath field and sheath width with respect to applied power.

$$E_b \approx \frac{J_e * m_e * \sqrt{\vartheta^2 + \omega^2}}{e^2 * n_e} \tag{2}$$

where, J_e denotes the conduction current due to electrons and ω is the applied excitation frequency (2*π*27.12 rad/s). The E_b increase monotonically with applied power, were depicted in **Fig. 3**. Since the amplitude of the 27.12 MHz electric field within the plasma enhances with the increase of externally applied power thus, the oscillating electrons gain enough energy from the electric field, as a result the bulk field would increase with applied power under constant chamber pressure. Other significant parameters related to the plasma discharge are sheath field and sheath width which can be evaluated using the discharge capacitive component (C). Sheath field is responsible for the acceleration of ions from the plasma bulk towards the substrate and also accountable for the growth and etching of the films whereas plasma density, ion energy and ion flux strongly affect the sheath width. Furthermore, reduced sheath thickness enhances the diffusion of high order Silane radicals (Si_2H_4, Si_3H_8, Si_2H_6, etc.), hence radical flux increases on the substrate. The sheath width can be calculated as;

$$d_s = \frac{A * \epsilon_o}{C} \quad (3)$$

where, A, ϵ_o and f are the area of electrode, absolute permittivity in vacuum and excitation frequency i.e. 27.12 MHz, respectively. **Fig. 3** shows the variation of sheath field and width with change in applied power. The sheath field increases from 947 V/cm to 1518 V/cm with the increase in power, the higher sheath field associated with the high energy of the ions accelerate towards the substrate. However, in the case of the growth of nc-Si:H, high energetic ions bombardment may disrupt the crystalline phase formation, hence the sheath field should be optimum for the crystalline nucleation. In addition to that minimum sheath width (7.1 x 10^{-4} cm) is observed at 20 W which corresponds to high radicals/ion flux with minimum ionic bombardment on the surface of the substrate.

In the present study, optimum bulk and sheath field and low sheath width was observed at 20 W applied power. As reported earlier, high density of ions/radicals and less ionic bombardment on the substrate are the preferred plasma conditions for the nucleation of nc-Si:H film [**15**]. For that reason, 20 W can be predicted as optimum power to obtain nc-Si:H according to plasma diagnosis and thus deposition has been carried out by variation of applied power from 4 W to 20 W.

Since the deposition rate of the film depends upon the electron density, ions/radicals flux, energy of the impinging ions, sticking coefficient, rate of surface chemical reaction, etc. It was found that deposition rate changes from 1.1 Å/s to 1.4 Å/s and 1.5 Å/s on 4 W, 10 W and 20 W applied power, respectively. The increase in deposition rate was in well correlation with the high bulk and sheath field and low sheath width due to which more number of ions accelerates towards the substrate. **Fig. 4** shows the Raman spectrum of the films deposited on 4 W - 20 W applied power.

At low power i.e. 4 W, a prominent peak observed near 480 cm^{-1} corresponds to transverse optical (TO) bands of Si-Si phonon vibration and reveals the amorphous nature of the film [**10**]. As the applied power increases further, TO peak shifts toward higher wave number this can be correlated with the presence of crystallites in the film. At 20 W power a peak observed at 516 cm^{-1} corresponding to TO vibration mode of nc-Si:H. To estimate X_c of nc-Si:H film deposited at 20 W, spectrum was de-convoluted into three peak, elucidate in **Fig. 4 (b)**. For this crystallite volume fraction is 24 % and crystallite size is 4.8 nm whereas at 10 W power peak observed at 484 cm^{-1} corresponds to mixed phase of a-Si:H and nc-Si:H. The Tauc's plots of the film deposit at different power shown in **Fig. 5**. The estimated values of direct Band gap (E_g) show in the inset of **Fig. 5**. The wider E_g (2.0 eV) observed at 20 W. Widening of E_g can be explained by existence of the nano-crystals, where these crystallites play significant role in transport property and film stability. The elevated absorption due to this results in shifting of curve towards the higher photon energy [**16**]. These results are in good agreement with the plasma diagnosis.

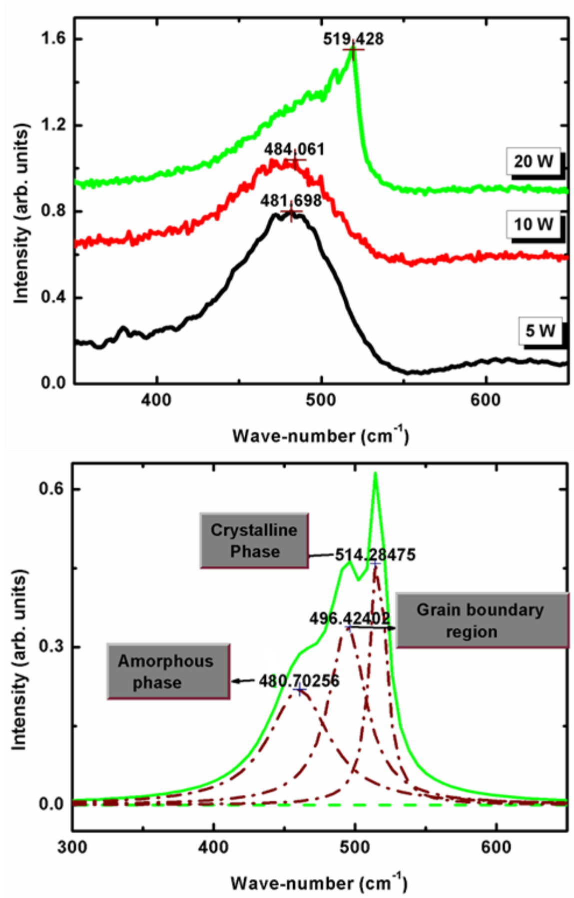

Fig. 4. Normalised Raman spectra of nc-Si:H/a-Si:H film deposited at different power.

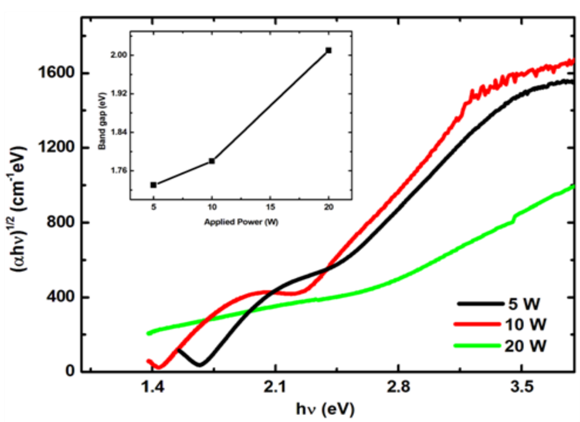

Fig. 5. Tauc's plot of optical absorption spectra in the UV-Vis range of film deposited at different power.

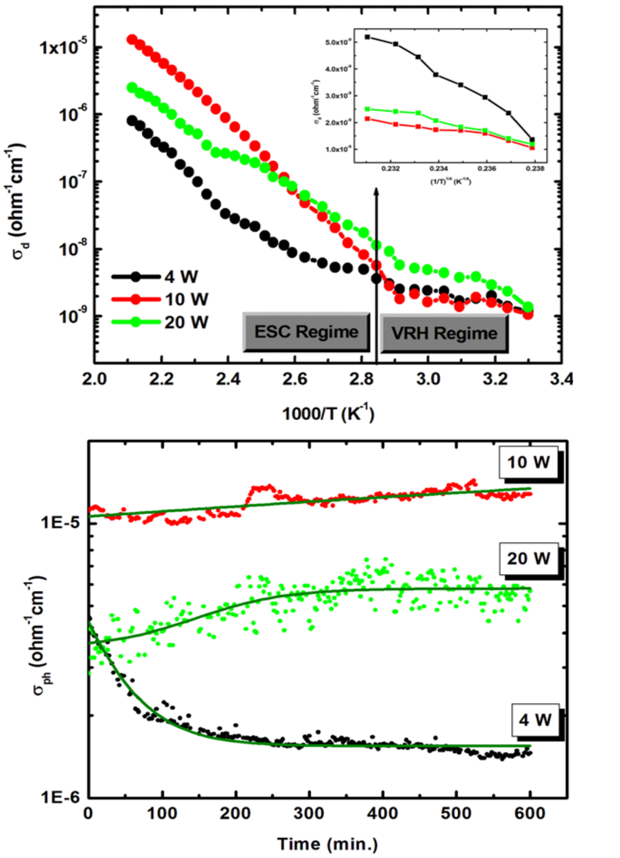

Fig.6 (a) Arrhenius plot of the temperature dependent dark conductivity of a-Si:H/nc-Si:H film deposited at different power (b) Photo-conductivity measurement of the film under 600 minutes of light soaking.

Electrical property can be estimated through dark conductivity (σ_d), photoconductivity (σ_{ph}), photo-gain (= $\sigma_{ph}/\ \sigma_d$) and activation energy (E_a). The values of photo-gain are 2.1 x 10^3, 7.2 x 10^3 and 3.6 x 10^2 at 4W, 10 W and 20 W applied power, respectively. The decrease of photo-gain may be associated with reduction of amorphous content in the film. To find the influence of power variation on the charge transport mechanism, the dc conductivity of the sample has been measured in the temperature range of 298-473 K. **Fig. 6(a)** shows the temperature dependent σ_d in which the plot was divided into two regime by the well-defined change in the slope at T = 338 K. Above 338 K, the region is associated with thermally activated carriers in a-Si:H, corresponds to the shift in Fermi level towards conduction band (Extended State Conduction (ESC) regime). Also, Variable Range Hopping (VRH) conduction appears conduction in these films at lower temperature (T < 338 K), originates from localised states where the electrons hop to a neighboring site [**17**]. The transport model for this is described as [**18**],

$$\sigma = \sigma_0 e^{\left(\frac{-E_a}{KT}\right)} - \sigma_1 e^{\left(\frac{-T_0}{T}\right)^{1/4}} \qquad (4)$$

where, σ_o, σ_1 is the conductivity prefactor, k is the Boltzmann constant, E_a is the activation energy of the extended states and T_o is the coefficient of the hopping process can be extracted by a linear relationship between ln σ_d vs. $T^{-1/4}$, as shown in the inset of **Fig. 6**. The estimated values of activation energy in the ESC region and T_o in the VRH region were 0.68 eV, 0.95 eV and 0.98 eV and 1.5 x 10^8 K , 6.7 x 10^8 K and 3.8 x 10^6 K at 4 W, 10 W and 20 W applied power, respectively. The low value of T_o in the VRH regime was found at 20 W which support the presence of minimum localized states in the nc-Si:H film. On the other hand, high value E_a in the ESC regime again predicts the presence of crystallites in the film. In order to obtain a better understanding of the stability of the film, light soaking measurements has been carried out for 600 min. under white light illumination of intensity~100 mW/cm^2. The results of the same are shown in **Fig. 6 (b)**. From these results, one can clearly see the film deposited at10 W and 20 W reflects a stable configuration, whereas film deposited at 4 W degrade up to 28 % from its initial photoconductivity value. It is reasonable to speculate that the existence of nano-crystals plays an important role in the stability. One may also say that the film deposit at 10 W have large amorphous component but still shows the stability comparable to the nc-Si:H. The small crystals with a reasonable amount of amorphous content may provide a compact material structure which reduces trap centers, as T_o in the VRH regime also indicates the same phenomena, might be the possible reason for this observation. Thus, we can say that the film deposited at and just after transition point is evidence for a better transport property and stability.

Conclusion

A process window for the growth of a-Si:H/ nc-Si:H films using 27.12 MHz assisted PECVD process was identified by precisely plasma monitoring though impedance analyzer. It is shown that at power 20 W, there was considerable change in the plasma characteristics denotes the nc-Si:H to a-Si:H transition region. For the better understanding of plasma parameter, the films were deposited under similar deposition conditions. Interestingly, correlation was observed among the plasma characteristics and film properties where the combination of low sheath width (7.4 x 10^{-4} cm) and high bulk field (5 V/cm) leads to existing crystalline phase in the amorphous film. In addition to that high quality a-Si:H in terms of deposition rate (1.39 Å/s), photo-gain (7.2 x 10^3) and stability observed just before transition. Thus, these films (a-Si:H and nc-Si:H) at the transition regime can be effectively utilized in fabrication of multi-junction solar cell for enhance efficiency and better stability.

Acknowledgements

The authors are grateful to Director, CSIR National Physical Laboratory, New Delhi (India) for his kind support. We are also thankful to Dr. Bhanu Pratap Singh from NPL, New Delhi for providing Raman Spectroscopy facility. Author also thankful to Kalpana Lodhi and Yamini Pant from NPL for the help during experiment. We also acknowledge CSIR-India for TAPSUN program and MNRE, Govt. of India for the research grant (sanction 31/29/2010-11/PVSE).

References

1. Kondo, M.; Matsuda, A.; Thin Solid Films, **2004**, 457, 97.
2. Guha, S.; Yang, J.;Yan, B.; Solar Energy Materials and Solar Cells, **2013**,119,1.
3. Chiu, IC.; Cheng, IC.; Chen, JZ.; Huang, JJ.; Chen, YP.; In MRS Proceedings **2011**,1321,11.
4. Gope, J.; Kumar, S.; Sudhakar, S.; Rauthan, CM.; Srivastava, PC.; Materials Chemistry and Physics, **2013**,141, 89**.**
5. Chowdhury, A.; Mukhopadhyay, S.; Ray, S.; Solar Energy Materials and Solar Cells, **2010**, 94, 1522.
6. Chengzhao, C.; Shenghua, Q.; Cuiqin, L.; Yandan, W.; Ping, L.; Chuying, Y.; Xuanying, L.; Plasma Science and Technology, **2009**, 11, 297.
7. Waman, V.S.; Mayabadi, A.H.; Kamble, M.M.; Gabhale, B.B.; Funde, A.M.; Sathe, V.G.; Pathan, H.M.; Jadkar, S.R.; Advanced materials letters, **2015**.
8. Yue, G.; Yan, B.; Ganguly, G.; Yang, J.; Guha, S.; Teplin, C.; Applied physics letters, **2006**, 88, 263507.
9. Godyak, V.A.; Piejak, R.B.; and Alexandrovich, B.M.;Plasma Science,**1991**, 19,660.
10. Wei, W.; Xu, G.; Wang, J.; Wang, T.; Vacuum, **2007**, 81, 656.
11. Richter, H.; Wang, Z.P.; Ley, L.; Solid State Communications, **1991**, 39, 625.
12. Balamurugan, B.; Mehta, B.R.; Thin solid films, **2001**, 396, 90.
13. Morgan, W. L.; Boeuf, J.P.; Pitchford, L.C.; "BOLSIG Boltzmann Solver." **1996**, Kinema Software, Monument, CO.
14. Parashar, A.; Kumar, S.; Dixit, P.N.; Gope, J., Rauthan, C.M.S.; Hashmi, S.A; Solar Energy Materials and Solar Cells,**2008**, 92,1199.
15. Sahu, B.B.; Han, J.G.; Shin, K.S.; Ishikawa, K.; Hori, M.; Miyawaki, Y.; Plasma Sources Science and Technology, **2015**, 24, 025019.
16. Funde, A.M.; Bakr, N.A.; Kamble, D.K.; Hawaldar, R.R.; Amalnerkar, D.P; Jadkar, S.R.; Solar Energy Materials and Solar Cells, **2008**, 92,1217.
17. Yildiz, A.; Serin, N.; Serin, T.; Kasap, M.; Japanese Journal of Applied Physics, **2009**, 48, 111203.
18. Chaudhary, D.; Sharma, M.; Sudhakar, S.; and Kumar, S.; Silicon, **2016**, 1.

